

Neutron single-particle states above the $N = 164$ subshell in ^{251}Cf and ^{249}Cm studied by neutron transfer reactions

I. Ahmad and R. R. Chasman

Physics Division, Argonne National Laboratory, Argonne, Illinois 60439, USA

(Received 9 November 2009; published 18 December 2009)

Single-particle state assignments in ^{251}Cf and ^{249}Cm at ~ 1 MeV excitation have been deduced from cross sections previously measured for the $^{250}\text{Cf}(d,p)^{251}\text{Cf}$ and $^{248}\text{Cm}(^4\text{He},^3\text{He})^{249}\text{Cm}$ reactions. The assignments are supported by observed cross-section signatures and intraband level spacings. The observed energies of these single-particle states, after pairing effects are removed, are in good agreement with values calculated using a Woods-Saxon single-particle potential. Neutron level diagrams, showing level spacings as a function of ν_2 , ν_4 , and ν_6 , are extended to include neutron orbitals above $N = 164$.

DOI: [10.1103/PhysRevC.80.064315](https://doi.org/10.1103/PhysRevC.80.064315)

PACS number(s): 21.10.Pc, 23.20.-g, 27.90.+b

I. INTRODUCTION

Large gaps and low-level density at the Fermi level provide extra stabilization for nuclei. When these conditions hold for both protons and neutrons in spherical nuclei, one has doubly magic nuclei. An equivalent situation arises in deformed nuclei, when there are large gaps in the single-particle spectra of protons and neutrons. In such cases, vibrational states are relatively high and single-particle states should be particularly pure. ^{252}Fm and ^{248}Cm are examples of a deformed doubly magic nucleus, as there are large gaps in the single-particle spectrum for protons at $Z = 96$ and $Z = 100$ and for neutrons at $N = 152$ [1]. Single-nucleon transfer reactions populating nuclei with ± 1 proton or neutron relative to these nuclides provide particularly good experimental tests of single-particle potentials. In ^{253}Fm , only two Nilsson states have been identified [2], because short lifetimes make that nucleus hard to access. Given present day experimental limitations, we can best study neutron single-particle states above the 152 neutron gap with spectroscopic studies of the $N = 153$ nuclide ^{249}Cm . ^{251}Cf is also stabilized by a low level density at $Z = 98$.

In addition to their intrinsic interest, the single-particle states above $N = 152$ largely define the level densities and gaps at $N = 184$, which is expected [3,4] to be a magic number for spherical nuclei. Specifically, the spherical $g_{7/2}$ and $d_{5/2}$ orbitals expected to be below the $N = 184$ spherical gap and the $h_{11/2}$ and $k_{17/2}$ spherical orbitals expected to be above the $N = 184$ gap give rise to deformed states that might be seen above $N = 152$. However, no deformed states in this region deriving from the spherical $d_{3/2}$ or the $s_{1/2}$ orbital are expected to be below the $N = 184$ gap. The stability of spherical superheavy nuclei arises from the large gap at $N = 184$ and the low level density above $N = 178$. Experimental measurements of level spacings at $N = 153$ provide a good test of potential parameters used to describe heavy and superheavy elements.

The $N = 153$ nuclei ^{249}Cm and ^{251}Cf are the heaviest nuclei for which single-neutron transfer reaction measurements have been performed. In both of these nuclides, the Nilsson orbital $1/2^+[620]$ is the ground state. Additionally, there are four (five) low-lying orbitals that can be accessed by one-neutron

transfer reactions up to the gap at $N = 162$ (164). The exact location of the gap depends sensitively on the values of the deformation parameters, as the energy of the $1/2^- [750]$ orbital changes rapidly with deformation, as has been shown in Figs. 5–7 of Ref. [1]. Single-particle states in these nuclei identified in many studies have already been published. In particular, in the $^{250}\text{Cf}(d,p)$ reaction [5], many low- j states have been identified in ^{251}Cf ; and in the $(^4\text{He},^3\text{He})$ reaction [6], high- j orbitals have been identified in ^{249}Cm . Since the publication of those studies, new measurements on levels in ^{251}Cf [7] and ^{249}Cm [8] have been performed. Making use of these new data, we have reanalyzed our (d,p) and $(^4\text{He},^3\text{He})$ reaction data and identified new states and confirmed previously assigned states.

II. EXPERIMENTAL DATA

The levels of ^{251}Cf have been studied in our laboratory for the past 35 yr with high-resolution α , electron, and γ -ray spectroscopy [7,9–11] and high-resolution neutron transfer reactions [5]. Decay scheme studies provide spins and parities of the states, and the (d,p) reaction gives information on the population of members of rotational bands which characterize the Nilsson-state assignments. From these studies, all of the predicted single-particle states below 800 keV excitation in ^{251}Cf have been identified. In our $^{250}\text{Cf}(d,p)$ spectrum [5], we found three strong peaks near 1 MeV at 972, 1183, and 1262 keV. In Ref. [5], we tentatively assigned the $9/2^+[604]$ and $1/2^- [761]$ configurations to bands at 1183 and 1250 keV, respectively. Recently, making use of γ -ray spectroscopic information [7], we deduced the spin-parity of the 974.0-keV level as $9/2^+$, and since the energy measured in the decay work matches the energy of the 972-keV level identified in the (d,p) reaction, we have assigned it as the $9/2^+[604]$ state. This assignment is further supported by the agreement between the measured and calculated cross sections for the $9/2^+[604]$ configuration. Accordingly, our tentative assignment of the $9/2^+[604]$ Nilsson state to the 1183-keV level is incorrect. Taking the new $9/2^+[604]$ assignment into account, we have reanalyzed our data and have identified the $3/2^- [752]$ Nilsson state for the first time, and we have

obtained additional evidence for the $1/2^-$ [761] band in ^{251}Cf . In this work, we present the measured cross sections for the $^{250}\text{Cf}(d,p)^{251}\text{Cf}$ reaction and compare them with values calculated with a distorted-wave Born approximation (DWBA) code.

The details of the $^{250}\text{Cf}(d,p)^{251}\text{Cf}$ reaction measurements have already been presented in Ref. [5]. In that paper, the spectra were displayed and the assignments deduced from the reaction data; earlier decay studies were also presented. Since then, the decay of ^{255}Fm was investigated [7] using a much stronger source and the Gammasphere spectrometer. These decay measurements confirmed the assignment of the $1/2^-$ [750] band to the 632.0-keV level and established the $9/2^+$ [604] state at 974.0 keV. Because the $9/2^+$ [604] Nilsson state has been assigned to the 974.0-keV level, we have assigned the remaining peaks in the 1-MeV region to other Nilsson states.

As discussed in Ref. [5], the (d,p) reaction preferentially populates particle states (states above the Fermi level with $U_K^2 > 0.5$). Also, the (d,p) reaction has larger cross sections for states with lower l values (0 to 4), and the cross section decreases with increasing l value. States that are expected to occur around 1 MeV excitation in ^{251}Cf are given in Ref. [6]. The two states calculated to have the largest cross sections are the $5/2$ member of the $1/2^-$ [761] band and the $7/2$ member of the $3/2^-$ [752] band. We assign these configurations to the strongest peaks in the spectrum, shown in Fig. 1, at 1183 and 1262 keV. These assignments are based on the calculated cross sections and the observation of other members of these bands in the spectra. Using the typical rotational constant of 6.5 keV, we determine the bandhead energies of the $1/2^-$ [761] and $3/2^-$ [752] bands as 1250 and 1105 keV, respectively.

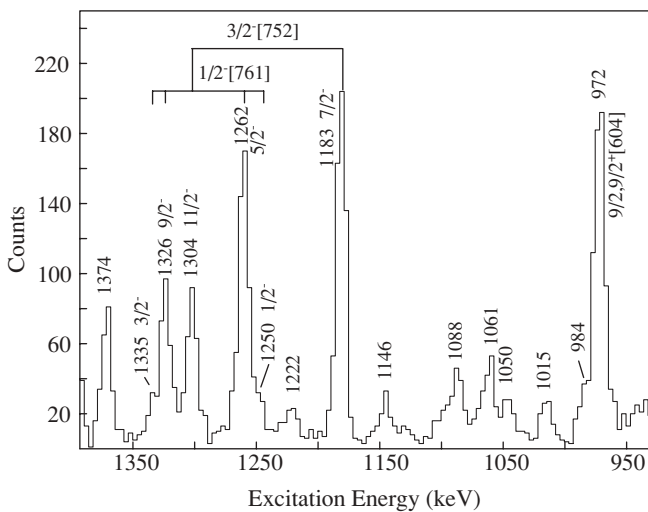


FIG. 1. Portion of the $^{251}\text{Cf}(d,p)^{251}\text{Cf}$ spectrum measured at 90° with an Enge split-pole magnetic spectrograph showing the levels in the 900–1400 keV region. This is the same spectrum as shown in Fig. 2 of Ref. [5], but plotted on a linear scale. The numbers on the peaks show the level energy and spin-parity assignment.

The differential cross section, $d\sigma/d\Omega$, for the (d,p) reaction at a given angle is given by the expression [12]

$$d\sigma/d\Omega = 2[(1.55\theta_{\text{DW}}/(2j+1))U_K^2 c_{jK}^2], \quad (1)$$

where θ_{DW} is the cross section for the spherical state with spin j calculated with the DWBA method, U_K^2 is the probability that the level K is unoccupied, and c_{jK} is the expansion coefficient of the deformed nuclear wave function in terms of the spherical basis states. For a given band, U_K^2 is the same for all its members, and hence the relative cross sections depend on θ_{DW} and c_{jK}^2 only. For the cross section calculation, θ_{DW} is computed with the DWBA code DWUCK4 [13], and the values of c_{jK}^2 and U_K^2 are obtained from Refs. [5] and [1]. In the literature, two sets of optical model potential parameters [14,15] have been used to calculate the cross sections in actinide nuclei. We have calculated the cross sections with the parameters of Ref. [14] because they give better agreement with data. The measured cross sections, values of U_K^2 and c_{jK}^2 , and DWBA cross sections needed for the calculation of cross sections are given in Table I. The last two columns contain the ratios of experimental and calculated cross sections at 90° and 120° . The uncertainties in cross sections represent statistical errors only. The uncertainties in the absolute cross sections are estimated to be $\sim 15\%$. The ratios at the two angles are equal when the cross sections follow the theoretical angular distributions. As the data show, for most of the levels, the angular distributions support the assignments. For many of the states, the theory reproduces the measured cross sections. For states with very small values of c_{jK}^2 , the theoretical cross sections have large uncertainties. The deviation between experimental and theoretical cross sections increases with increasing transferred angular momentum as has been observed in other nuclei [14].

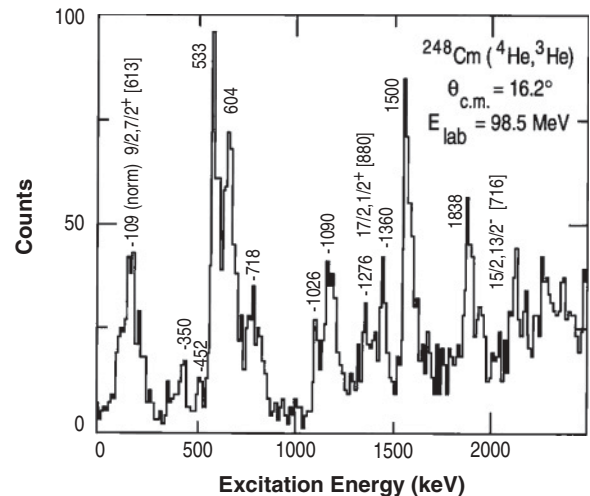


FIG. 2. Portion of the $^{248}\text{Cm}(^4\text{He},^3\text{He})^{248}\text{Cm}$ spectrum measured with a magnetic spectrometer at 16.2° with a beam energy of 98.5 MeV. This is the same spectrum as shown in Fig. 5 of Ref. [6], but the level energies are determined by normalizing to the 109-keV energy of the $9/2, 7/2^+$ [613] level. The relative uncertainties in level energies are ± 5 keV. The assignments of the 109-, 1500-, and 1838-keV peaks are shown in the figure; other assignments are discussed in the text.

TABLE I. Comparison of measured and theoretical cross sections for the $^{250}\text{Cf}(d,p)^{251}\text{Cf}$ reaction. Parameters of the DWBA code were taken from Ref. [11]. Note that $d\sigma/d\Omega = 3.1[\theta_{\text{DW}}/(2j+1)]U_K^2 c_{jK}^2$.

Orbital $K^\pi [Nn_z\Delta]$	Energy (keV)	Spin \hbar	$(d\sigma/d\Omega)_{\text{exp}}$		$\theta_{\text{DW}}/(2j+1)$ 90° ($\mu\text{b}/\text{sr}$)	Theory		$(d\sigma/d\Omega)_{\text{exp}}/(d\sigma/d\Omega)_{\text{th}}$	
			90° ($\mu\text{b}/\text{sr}$)	120° ($\mu\text{b}/\text{sr}$)		U_K^2	c_{jK}^2	90°	120°
1/2 ⁺ [620]	0	1/2	278(13)	189(7)	525	0.90	0.13	1.46(7)	1.44(6)
	24	3/2	17(3)	12(2)	242	0.90	0.041	0.61(11)	0.47(8)
	48	5/2	133(7)	126(6)	243	0.90	0.209	0.94(5)	0.96(5)
	106	7/2	50(4)	55(4)	59.3	0.90	0.22	1.37(11)	1.29(10)
	146	9/2	34(4)	43(4)	59.9	0.90	0.24	0.85(10)	0.91(9)
	240	11/2	3.6(1.5)	4.2(1.5)	4.6	0.90	0.13	2.1(9)	1.2(5)
	292	13/2		~3	9.4	0.90	0.114		~3.8
7/2 ⁺ [613]	166	9/2	142(8)	183(7)	60.2	0.93	0.84	0.97(6)	1.06(4)
3/2 ⁺ [622]	177	3/2	125(6)	115(6)	258	0.95	0.17	0.97(5)	0.96(5)
	212	5/2	88(13)	56(4)	260	0.95	0.091	1.26(19)	0.86(7)
	258	7/2	63(5)	68(5)	61.5	0.95	0.36	0.97(8)	0.88(7)
	318	9/2	56(5)	70(6)	62.3	0.95	0.16	1.91(17)	1.99(17)
5/2 ⁺ [622]	544	5/2	9(2)	7.0(1.5)	295	0.04	0.071	3.5(8)	2.8(6)
	649	9/2	22(5)	32(3)	67.2	0.04	0.65	4.1(10)	4.8(5)
11/2 ⁻ [725]	569	15/2	21(4)	34(3)	1.44	0.90	0.98	5.3(10)	3.0(3)
1/2 ⁻ [750]	632	1/2	99(10)	95(6)	404	0.97	0.031	2.6(3)	3.0(2)
	600	3/2	269(10)	213(8)	398	0.97	0.18	1.25(5)	1.19(5)
	708	5/2	12(3)		125	0.97	0.039	0.82(21)	
	625	7/2	278(10)	280(10)	122	0.97	0.38	1.99(8)	1.80(7)
	691	11/2	58(10)	69(5)	13.5	0.97	0.207	6.9(12)	5.2(4)
	775	15/2	~2		1.43	0.97	0.12	~4	
9/2 ⁺ [615]	683	9/2	69(10)	80(5)	67.7	0.90	0.069	5.3(8)	4.9(3)
	758	11/2	36(4)		4.8	0.90	0.91	3.0(4)	
9/2 ⁺ [604]	972	9/2	126(10)	150(9)	72.3	0.97	0.91	0.64(5)	0.59(4)
3/2 ⁻ [752]	1183	7/2	150(10)	188(10)	162	0.98	0.309	0.99(7)	1.06(6)
	1304	11/2	61(5)	97(7)	15.8	0.98	0.29	4.4(4)	4.0(3)
1/2 ⁻ [761]	1250	1/2	22(3)	27(3)	539	0.98	0.031	0.43(6)	0.59(7)
	1335	3/2	15(3)	~16	557	0.98	0.003	2.9(6)	~2.8
	1262	5/2	112(10)	124(8)	155	0.98	0.186	1.28(12)	1.23(8)
	1326	9/2	63(7)	103(7)	9.8	0.98	0.347	6.1(7)	5.6(4)

The level structure of ^{249}Cm has been studied by the $^{248}\text{Cm}(d,p)$ reaction [15], $^{248}\text{Cm}(n,\gamma)$ reaction [16], $^{248}\text{Cm}(^4\text{He},^3\text{He})$ reaction [6], and $^{248}\text{Cm}(\text{HI},\gamma)$ spectroscopy [8]. High- j states in ^{249}Cm were identified in the ($^4\text{He},^3\text{He}$) reaction. Precise energies of these levels were measured in recent γ -ray spectroscopic studies [8].

The energy of the $I, K^\pi [Nn_z\Delta] = 17/2, 1/2^+ [880]$ state was found to be 1505(2) keV in the recent $^{248}\text{Cm}(\text{HI},\gamma)$ spectroscopy measurement [8], which is 55 keV lower than the value of 1560 keV measured in the ($^4\text{He},^3\text{He}$) reaction [6]. In the ($^4\text{He},^3\text{He}$) reaction, the level energies were determined as absolute energies from the ^4He beam energy and the energy of the emerging ^3He ions measured with a magnetic spectrometer. Since the beam energy was quite high (98.5 MeV), the deduced level energies had large uncertainties. We have now determined the energies of the peaks in the spectrum relative to the known energy of the 9/2, 7/2⁺[613] level. The energies so determined are shown in Fig. 2. The new energy of the 17/2, 1/2⁺[880] level is 1500 keV, in excellent agreement with the value reported by Ishii *et al.* [8]. The agreement between the two measurements provides confidence in the assignment of the 1/2⁺[880] state, because the 1/2⁺[880] orbital is mostly

$k_{17/2}$. Additional support for this assignment comes from a likely identification of its $I = 13/2$ member at 1360 keV in our $^{248}\text{Cm}(^4\text{He},^3\text{He})$ spectrum shown in Fig. 2.

The energies of the other strong peaks in Fig. 2 fit well with energies of the bandheads determined in Ref. [8]. Because of the large cross section, the peak at 1838 keV has been assigned to the 15/2, 13/2⁻[716] level. The peaks at 533 and 604 keV are assigned to the 15/2, 11/2⁻[725] and 11/2, 9/2⁺[615] configurations, respectively. These assignments in conjunction with the energies of bandheads reported in Ref. [8] give reasonable values of rotational constants of 5.6 and 6.5 keV for the 11/2⁻[725] and 9/2⁺[615] bands. From the energy of the 15/2 member and a rotational constant of 6.5 keV, we determine the energy of the 13/2⁻[716] bandhead as 1740 keV.

III. DISCUSSION

Because nuclides having more neutrons than we had envisioned 30 yr ago will soon be experimentally accessible for spectroscopic studies, we have extended our plot [1] of neutron single-particle levels as a function of deformation to

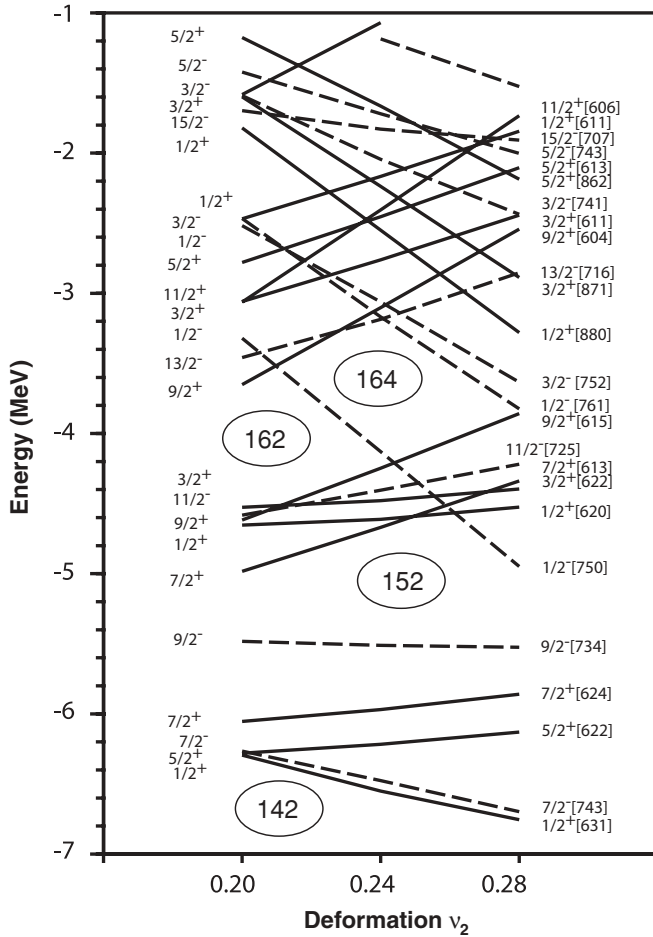


FIG. 3. Neutron single-particle energies calculated with a Woods-Saxon potential in ^{249}Cm as a function of deformation parameter ν_2 . The values of ν_4 and ν_6 were fixed at 0.0. Solid lines represent positive-parity states and dashed lines negative-parity states.

$N \sim 190$. These plots are centered at $\nu_2 = 0.24$, $\nu_4 = 0.0$, and $\nu_6 = 0.0$, where ν_2 is a quadrupole deformation parameter, ν_4 is a hexadecapole deformation parameter, and ν_6 is a 2^6 -pole deformation. Exact definitions of these deformation parameters are given in Ref. [1], Appendix A. In Figs. 3–5, we present plots of the energies of single-particle neutron states as a function of deformations ν_2 , ν_4 , and ν_6 . These were calculated with the Woods-Saxon potential parameters of Ref. [17] for $A = 250$, and these differ slightly from those of Ref. [1]. These plots suggest that spectroscopic studies of nuclei with 163 and 165 neutrons will be interesting as four or five (depending on the exact values of deformation parameters) single-particle states will be comparatively pure and low-lying because $N = 162$ and $N = 164$ are deformed magic numbers.

In Fig. 6, we compare the extracted experimental level energies with the theoretical values calculated with the potential parameters of Ref. [17]. The comparison for levels below 800 keV has been discussed in Refs. [5] and [6]. As Fig. 6 shows, the experimental energies are in good agreement with theoretical values. Calculations using beyond

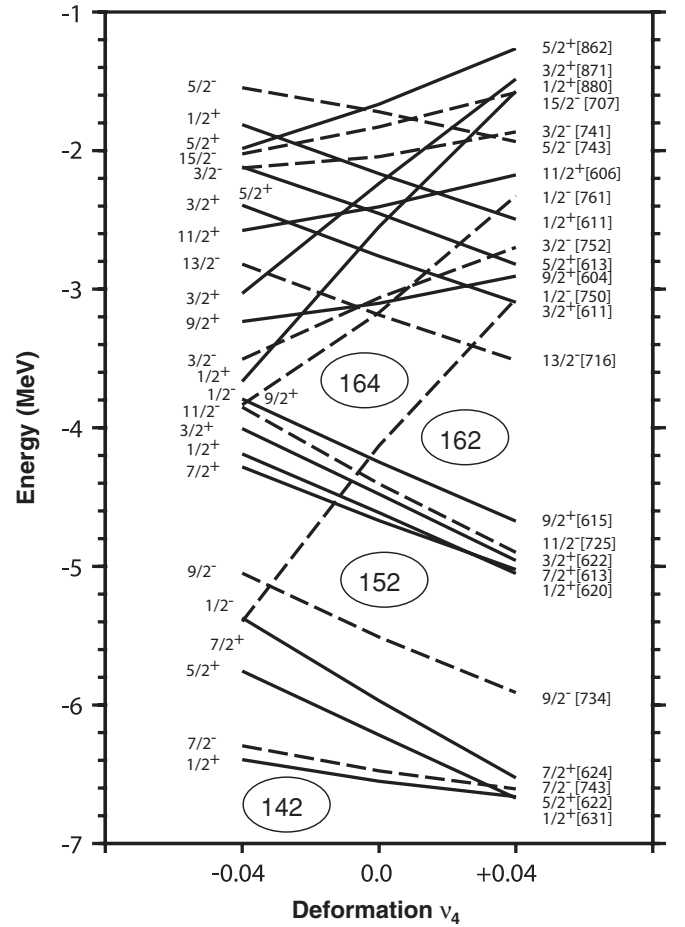


FIG. 4. Neutron single-particle energies calculated with a Woods-Saxon potential in ^{249}Cm as a function of deformation parameter ν_4 . The values of ν_2 and ν_6 were fixed at 0.24 and 0.0, respectively. Solid lines represent positive-parity states and dashed lines negative-parity states.

the mean field are needed to determine the extent to which the excitation energy of the $1/2^+[880]$ orbital is lowered by its deformation-driving nature.

The $1/2^+[880]$ band has a large Coriolis matrix element with the $3/2^+[871]$ band, and it also has a large decoupling parameter. The measured energy of 1505 keV for the $17/2$ level is lower than the energy of the unmixed state. We have estimated the contribution of the Coriolis mixing using our calculated level energies and Coriolis matrix elements [5]. We find that the Coriolis mixing lowers the energy of the $17/2$ member of the $1/2^+[880]$ band by ~ 200 keV. Thus the energy of the unmixed $17/2$, $1/2^+[880]$ level should be 1705 keV, which gives the energy of the bandhead as 1600 keV. This value is shown in Fig. 6.

IV. SUMMARY

Three new single-particle states in ^{251}Cf and two new states in ^{249}Cm above the $N = 164$ subshell have been

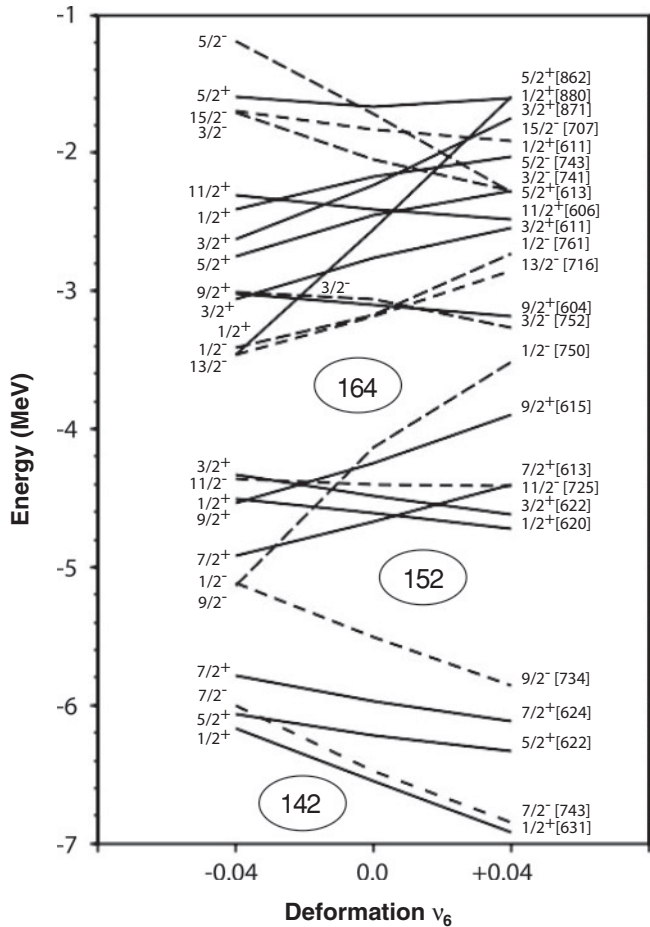


FIG. 5. Neutron single-particle energies calculated with a Woods-Saxon potential in ^{249}Cm as a function of deformation parameter ν_6 . The values of ν_2 and ν_4 were fixed at 0.24 and 0.0, respectively. Solid lines represent positive-parity states and dashed lines negative-parity states.

identified. These assignments had been suggested in our earlier publications, but the present paper provides additional evidence for them. The fact that the measured energies of these orbitals, which are expected to be the ground states of transactinide nuclides, are in good agreement with values calculated with our single-particle model provides support for the choice of potential parameters.

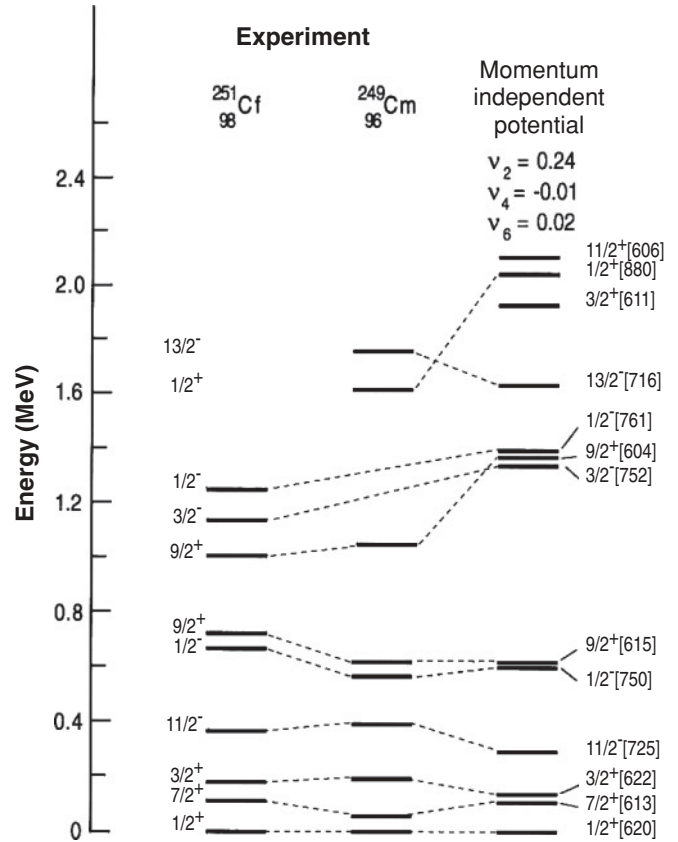


FIG. 6. Comparison of the experimental and theoretical level energies in ^{251}Cf and ^{249}Cm . Theoretical energies are taken from Ref. [6] and were calculated with a momentum-independent Woods-Saxon potential. The data represent the experimental bandhead energies and were obtained from the measured energies by removing the contributions from pairing interaction. This figure is a newer version of Fig. 8 of Ref. [6].

ACKNOWLEDGMENTS

We thank S. Zhu for his help in data analysis. We are indebted for the use of ^{248}Cm and ^{250}Cf to the Office of Basic Energy Sciences, US Department of Energy, through the transplutonium element production facilities at Oak Ridge National Laboratory. This work was supported by the US Department of Energy, Office of Nuclear Physics, under Contract No. DE-AC02-06CH11357.

- [1] R. R. Chasman, I. Ahmad, A. M. Friedman, and J. R. Erskine, Rev. Mod. Phys. **49**, 833 (1977).
- [2] M. Asai *et al.*, Phys. Rev. Lett. **95**, 102502 (2005).
- [3] A. Sobczewski, F. A. Gareev, and B. N. Kalinkin, Phys. Lett. **22**, 500 (1966).
- [4] H. Meldner, Ark. Fys. **36**, 593 (1967).
- [5] I. Ahmad, R. R. Chasman, A. M. Friedman, and S. W. Yates, Phys. Lett. **B251**, 338 (1990).
- [6] I. Ahmad *et al.*, Nucl. Phys. **A646**, 175 (1999).

- [7] I. Ahmad, J. P. Greene, E. F. Moore, F. G. Kondev, R. R. Chasman, C. E. Porter, and L. K. Felker, Phys. Rev. C **72**, 054308 (2005).
- [8] T. Ishii *et al.*, Phys. Rev. C **78**, 054309 (2008).
- [9] I. Ahmad, F. T. Porter, M. S. Freedman, R. F. Barnes, R. K. Sjblom, F. Wagner, Jr., J. Milsted, and P. R. Fields, Phys. Rev. C **3**, 390 (1971).
- [10] I. Ahmad and J. Milsted, Nucl. Phys. **A239**, 1 (1975).

- [11] I. Ahmad *et al.*, Phys. Rev. C **62**, 064302 (2000).
- [12] D. G. Burke, B. Zeidman, B. Elbek, B. Herskind, and M. Olesen, Mat. Fys. Medd. K. Dan. Vidensk. Selsk. **35**, 2 (1966).
- [13] P. D. Kunz and E. Rost, University of Colorado, code DWUCK4.
- [14] J. R. Erskine, Phys. Rev. C **5**, 959 (1972).
- [15] T. H. Braid, R. R. Chasman, J. R. Erskine, and A. M. Friedman, Phys. Rev. C **4**, 247 (1971).
- [16] R. W. Hoff, W. F. Davidson, D. D. Warner, H. G. Börner, and T. von Egidy, Phys. Rev. C **25**, 2232 (1982).
- [17] R. R. Chasman and I. Ahmad, Phys. Lett. **B392**, 255 (1997).